https://doi.org/10.5194/egusphere-2026-2653
Preprint. Discussion started: 11 June 2026

Estimating cross-correlation parameters between forecast and observation errors within the ensemble transform Kalman filter with cross correlation (ETKFCC)

Yuki Kobayashi[1], Shun Ohishi[2,3], Takemasa Miyoshi[2,3]

[1]Department of Environmental Engineering, Graduate School of Engineering, Kyoto University, Kyoto, 615-8540, Japan
[2]RIKEN Center for Computational Science, Kobe, 650-0047, Japan
[3]RIKEN Center for Interdisciplinary Theoretical and Mathematical Sciences (iTHEMS), Kobe, 650-0047, Japan

Correspondence to: Yuki Kobayashi (kobayashi.yuki.58w@st.kyoto-u.ac.jp)

Abstract. The Kalman filter (KF) and the ensemble KF (EnKF) are formulated under the assumption of no cross-correlation between the forecast and observation errors. However, some data assimilation systems assimilate analysis products such as optimal interpolation analyses and satellite retrievals, which may contain errors correlated with the forecast errors. The authors' previous study extended the KF and the ensemble transform KF (ETKF) to account for the cross-correlation (KFCC and ETKFCC, respectively) and demonstrated that the ETKFCC significantly outperforms the ETKF using the Lorenz-96 model. However, these experiments assumed that the cross-correlation parameters were perfectly known although they are unknown in practice. In this study, we extended the previous study by proposing a novel method to estimate the cross-correlation parameters from innovation statistics. We performed three experiments: (i) ETKFCC with estimated parameters, (ii) ETKFCC with prescribed true parameters, and (iii) ETKF. The results showed that the parameters were estimated well for positive cross-correlations, but not for unlikely cases of negative cross-correlations. For positive cross-correlations, the ETKFCC with the estimated parameters significantly outperforms the ETKF and is comparable to the ETKFCC with the prescribed true parameters when the cross-correlation is 0.2–0.7.

1 Introduction

Data assimilation combines simulations and observations based on statistical methods and dynamical systems theory to find the optimal analyses, estimate tunable parameters, and evaluate observing networks. There are various data assimilation methods such as the three- and four-dimensional variational methods (3D- and 4D-VAR, respectively), Kalman filter (KF), and ensemble Kalman filter (EnKF). These methods assume no cross-correlation between the forecast and observation errors. However, some practical data assimilation systems assimilate optimally interpolated observations in the ocean (e.g., Kido et al., 2022; Hirose et al., 2019) and reanalysis data in the atmosphere (Hoover and Langland, 2017). If the optimally interpolated data and reanalysis data include the same observations assimilated in the systems, the forecast errors may not be independent of the observation errors. In these cases, the forecast errors might contaminate the observation errors.

https://doi.org/10.5194/egusphere-2026-2653
Preprint. Discussion started: 11 June 2026

In the authors' previous study (Ohishi et al., 2025; hereafter simply "OKM25"), we proposed new formulations for the KF and ensemble transform Kalman filter (ETKF) with the cross-correlation (KFCC and ETKFCC, respectively). Using perfect-model twin experiments with the Lorenz-96 model (Lorenz, 1996; Lorenz and Emanuel, 1998), we demonstrated that the ETKFCC is significantly more accurate than the standard ETKF, especially when the correlation coefficients are between 0.2 and 0.8, with negligible additional computational cost. In these experiments, observation errors correlated with the forecast errors were generated by adding a fraction of the forecast errors to independent random Gaussian noise [cf. eq. (1) of OKM25; Eq. (1) in Sect. 2a], and the parameters for the fraction of the forecast errors $\mathbf{A}$ and the noise variance $\mathbf{R}^{uc}$ were assumed to be known. In practice, however, the cross-correlations between forecast and observation errors cannot be directly estimated because true state values are unknown. To solve this problem, this study extends OKM25 by introducing a novel method to estimate the cross-correlation parameters from innovation statistics (Desroziers et al., 2005), validating the estimated parameters, and comparing the analysis accuracy of the ETKFCC with the estimated parameters to that of the ETKFCC with the prescribed true parameters and the standard ETKF, using the Lorenz-96 model under the perfect model assumption.

In this paper, Sect. 2 describes the details of the observation errors correlated with the forecast errors, the formulations of the KFCC and ETKFCC, and the parameter estimation method based on innovation statistics. The experimental settings are described in Sect. 3. Sections 4 and 5 present the results and discussion, respectively, followed by a summary in Sect. 6.

2 Methods

2.1 Correlated observation errors with forecast errors

This study adopts the method of OKM25 to generate the observation errors $\boldsymbol{\epsilon}^o$ correlated with the forecast errors $\boldsymbol{\epsilon}^f$ as

$$\boldsymbol{\epsilon}^o = \mathbf{A}H(\boldsymbol{\epsilon}^f) + \boldsymbol{\eta}\,, \tag{1}$$

where $\mathbf{A} = diag(a_i)$ is a diagonal matrix with a_i $(i = 1, \ldots, p)$ being a scalar parameter, p the number of observations, H an observational operator, and $\boldsymbol{\eta}$ a Gaussian random noise with mean $\mathbf{0}$ and error covariance matrix $\mathbf{R}^{uc}$. Since $\boldsymbol{\eta}$ is independent of the forecast errors $\boldsymbol{\epsilon}^f$,

$$\langle \boldsymbol{\epsilon}^f \boldsymbol{\eta}^{\mathrm{T}} \rangle = \mathbf{O}\,. \tag{2}$$

Hereafter, the notations of symbols follow Tables A1–A6 in Appendix A.

https://doi.org/10.5194/egusphere-2026-2653
Preprint. Discussion started: 11 June 2026

2.2 Kalman filter and ensemble transform Kalman filter with the cross-correlation between the forecast and observation errors

As shown in OKM25, the KFCC is formulated as

$$\boldsymbol{x}^a = \boldsymbol{x}^f + \acute{\mathbf{K}}(\boldsymbol{y} - \mathbf{H}\boldsymbol{x}^f) \,, \tag{3}$$

$$\acute{\mathbf{K}} = (\rho\mathbf{P}^f\mathbf{H}^{\mathrm{T}} - \mathbf{C})(\rho\mathbf{H}\mathbf{P}^f\mathbf{H}^{\mathrm{T}} - \mathbf{H}\mathbf{C} - \mathbf{C}^{\mathrm{T}}\mathbf{H}^{\mathrm{T}} + \mathbf{R})^{-1} \text{ , and} \tag{4}$$

$$\acute{\mathbf{P}}^a = \rho\left(\mathbf{I}^{n\times n} - \acute{\mathbf{K}}\mathbf{H}\right)\mathbf{P}^f + \acute{\mathbf{K}}\mathbf{C}^{\mathrm{T}} \,, \tag{5}$$

where we note that acutes indicate including the cross-correlation between the forecast and observation errors. From the correlated observation errors [Eq. (1)] and no cross-correlation between the forecast errors and Gaussian random noise [Eq. (2)], $\mathbf{C} \cong \rho\mathbf{P}^f\mathbf{H}^{\mathrm{T}}\mathbf{A}^{\mathrm{T}}$ and $\mathbf{R} \cong \rho\mathbf{A}\mathbf{H}\mathbf{P}^f\mathbf{H}^{\mathrm{T}}\mathbf{A}^{\mathrm{T}} + \mathbf{R}^{uc}$. Substituting them into Eqs. (4) and (5), $\acute{\mathbf{K}}$ and $\acute{\mathbf{P}}^a$ can be represented as

$$\acute{\mathbf{K}} = \rho\mathbf{P}^f\mathbf{H}^{\mathrm{T}}(\mathbf{I}^{p\times p} - \mathbf{A})^{\mathrm{T}}[\rho(\mathbf{I}^{p\times p} - \mathbf{A})\mathbf{H}\mathbf{P}^f\mathbf{H}^{\mathrm{T}}(\mathbf{I}^{p\times p} - \mathbf{A})^{\mathrm{T}} + \mathbf{R}^{uc}]^{-1} \text{ , and} \tag{6}$$

$$\acute{\mathbf{P}}^a = \rho\left[\mathbf{I}^{n\times n} - \acute{\mathbf{K}}(\mathbf{I}^{p\times p} - \mathbf{A})\mathbf{H}\right]\mathbf{P}^f \,. \tag{7}$$

Since the KFCC has similar forms to the standard KF, the ETKFCC is derived in the same way as the previous studies (e.g., Bishop et al., 2001):

$$\boldsymbol{x}^{a(i)} = \overline{\boldsymbol{x}}^f + \delta\mathbf{X}^f\left[\widetilde{\mathbf{P}}^a(\delta\mathbf{Y}^f)^{\mathrm{T}}(\mathbf{I}^{p\times p} - \mathbf{A})^{\mathrm{T}}(\mathbf{R}^{uc})^{-1}(\boldsymbol{y} - \mathbf{H}\overline{\boldsymbol{x}}^f) + \acute{\mathbf{W}}^{(i)}\right], \tag{8}$$

$$\widetilde{\mathbf{P}}^a = [(m-1)\,\mathbf{I}^{m\times m}/\rho + (\delta\mathbf{Y}^f)^{\mathrm{T}}(\mathbf{I}^{p\times p} - \mathbf{A})^{\mathrm{T}}(\mathbf{R}^{uc})^{-1}(\mathbf{I}^{p\times p} - \mathbf{A})\delta\mathbf{Y}^f]^{-1} \text{ , and} \tag{9}$$

$$\acute{\mathbf{W}} = \left[(m-1)\widetilde{\mathbf{P}}^a\right]^{1/2} \,. \tag{10}$$

See OKM25 for the detailed derivations. In the case of no cross-correlation (i.e., $\mathbf{A} = \mathbf{O}$), these formulations are consistent with the standard ETKF as shown below:

$$\boldsymbol{x}^{a(i)} = \overline{\boldsymbol{x}}^f + \delta\mathbf{X}^f\left[\widetilde{\mathbf{P}}^a(\delta\mathbf{Y}^f)^{\mathrm{T}}\mathbf{R}^{-1}(\boldsymbol{y} - \mathbf{H}\overline{\boldsymbol{x}}^f) + \mathbf{W}^{(i)}\right], \tag{11}$$

$$\widetilde{\mathbf{P}}^a = [(m-1)\,\mathbf{I}^{m\times m}/\rho + (\delta\mathbf{Y}^f)^{\mathrm{T}}\mathbf{R}^{-1}\delta\mathbf{Y}^f]^{-1} \text{ , and} \tag{12}$$

$$\mathbf{W} = \left[(m-1)\widetilde{\mathbf{P}}^a\right]^{1/2} \,. \tag{13}$$

https://doi.org/10.5194/egusphere-2026-2653
Preprint. Discussion started: 11 June 2026

2.3 Innovation statistics with the cross-correlation between the forecast and observation errors

In this study, $\mathbf{A}$ and $\mathbf{R}^{uc}$ are prescribed to generate the correlated observation errors [Eq. (1)], but they are unknown in practice. To estimate these parameters, we extend the innovation statistics formulation (Desroziers et al., 2005) to include the cross-correlation between the forecast and observation errors (see Appendix B for details). The estimated parameters are then substituted into the ETKFCC equations [Eqs. (8)–(10)].

The differences among the forecasts, analyses, and correlated observations in observation space are defined as

$$\boldsymbol{d}^{o-b} \equiv \boldsymbol{y} - H(\boldsymbol{x}^f) \cong \boldsymbol{\epsilon}^o - \mathbf{H}\boldsymbol{\epsilon}^f \,, \tag{14}$$

$$\boldsymbol{d}^{a-b} \equiv H(\boldsymbol{x}^a) - H(\boldsymbol{x}^f) \cong \mathbf{H}\acute{\mathbf{K}}\boldsymbol{d}^{o-b} \text{ , and} \tag{15}$$

$$\boldsymbol{d}^{o-a} \equiv \boldsymbol{y} - H(\boldsymbol{x}^a) \cong \left(\mathbf{I}^{p\times p} - \mathbf{H}\acute{\mathbf{K}}\right)\boldsymbol{d}^{o-b} \,. \tag{16}$$

As detailed in Appendix B,

$$\acute{\mathbf{K}}(\mathbf{R} - \mathbf{HC}) = \acute{\mathbf{P}}^a\mathbf{H}^{\mathrm{T}} - \mathbf{C} \,, \tag{17}$$

$$\acute{\mathbf{K}}(\rho\mathbf{HP}^f - \mathbf{C}^{\mathrm{T}}) = \rho\mathbf{P}^f - \acute{\mathbf{P}}^a \,. \tag{18}$$

Using Eqs. (14)–(18), innovation statistics with the cross-correlation are

$$\langle \boldsymbol{d}^{o-b}(\boldsymbol{d}^{o-b})^{\mathrm{T}} \rangle = \mathbf{R} - \mathbf{HC} - \mathbf{C}^{\mathrm{T}}\mathbf{H}^{\mathrm{T}} + \rho\mathbf{HP}^f\mathbf{H}^{\mathrm{T}} \,, \tag{19}$$

$$\langle \boldsymbol{d}^{a-b}(\boldsymbol{d}^{o-b})^{\mathrm{T}} \rangle = -\mathbf{HC} + \rho\mathbf{HP}^f\mathbf{H}^{\mathrm{T}} \,, \tag{20}$$

$$\langle \boldsymbol{d}^{o-a}(\boldsymbol{d}^{o-b})^{\mathrm{T}} \rangle = \mathbf{R} - \mathbf{C}^{\mathrm{T}}\mathbf{H}^{\mathrm{T}} \text{ , and} \tag{21}$$

$$\langle \boldsymbol{d}^{a-b}(\boldsymbol{d}^{o-a})^{\mathrm{T}} \rangle = \mathbf{H}\acute{\mathbf{P}}^a\mathbf{H}^{\mathrm{T}} - \mathbf{HC} \,. \tag{22}$$

Substituting $\mathbf{C} \cong \rho\mathbf{AHP}^f$ and $\mathbf{R} \cong \rho\mathbf{AHP}^f\mathbf{H}^{\mathrm{T}}\mathbf{A}^{\mathrm{T}} + \mathbf{R}^{uc}$ into Eqs. (19)–(22), the innovation statistics with the cross-correlation become

$$\langle \boldsymbol{d}^{o-b}(\boldsymbol{d}^{o-b})^{\mathrm{T}} \rangle = \rho(\mathbf{I}^{p\times p} - \mathbf{A})\mathbf{HP}^f\mathbf{H}^{\mathrm{T}}(\mathbf{I}^{p\times p} - \mathbf{A})^{\mathrm{T}} + \mathbf{R}^{uc} \,, \tag{23}$$

$$\langle \boldsymbol{d}^{a-b}(\boldsymbol{d}^{o-b})^{\mathrm{T}} \rangle = \rho\mathbf{HP}^f\mathbf{H}^{\mathrm{T}}(\mathbf{I}^{p\times p} - \mathbf{A})^{\mathrm{T}} \,, \tag{24}$$

$$\langle \boldsymbol{d}^{o-a}(\boldsymbol{d}^{o-b})^{\mathrm{T}} \rangle = -\rho\mathbf{AHP}^f\mathbf{H}^{\mathrm{T}}(\mathbf{I}^{p\times p} - \mathbf{A})^{\mathrm{T}} + \mathbf{R}^{uc} \text{ , and} \tag{25}$$

$$\langle \boldsymbol{d}^{a-b}(\boldsymbol{d}^{o-a})^{\mathrm{T}} \rangle = -\rho\mathbf{HP}^f\mathbf{H}^{\mathrm{T}}\mathbf{A}^{\mathrm{T}} + \mathbf{H}\acute{\mathbf{P}}^a\mathbf{H}^{\mathrm{T}} \,. \tag{26}$$

https://doi.org/10.5194/egusphere-2026-2653
Preprint. Discussion started: 11 June 2026

In the case of no cross-correlation (i.e., $\mathbf{A} = \mathbf{O}$), these formulations are consistent with the original innovation statistics (Desroziers et al., 2005).

Since Eqs. (24) and (26) depend on $\mathbf{A}$ but not on $\mathbf{R}^{uc}$, the diagonal components of $\mathbf{A}^{est} = diag(a_i^{est})$ $(i = 1, \dots, p)$ can be estimated as

$$a_i^{est} = 1 - \frac{\langle \boldsymbol{d}^{a-b}(\boldsymbol{d}^{o-b})^{\mathrm{T}} \rangle_{ii}}{\rho(\mathbf{H}\mathbf{P}^{f}\mathbf{H}^{\mathrm{T}})_{ii}} \text{ and} \tag{27}$$

$$a_i^{est} = \frac{(\mathbf{H}\mathbf{P}^{\acute{a}}\mathbf{H}^{\mathrm{T}})_{ii} - \langle \boldsymbol{d}^{a-b}(\boldsymbol{d}^{o-a})^{\mathrm{T}} \rangle_{ii}}{\rho(\mathbf{H}\mathbf{P}^{f}\mathbf{H}^{\mathrm{T}})_{ii}}, \tag{28}$$

respectively. If a_i^{est} is uniform (i.e., $\mathbf{A}^{est} = a^{est}\mathbf{I}^{p\times p}$), Eqs. (27) and (28) reduce to

$$a^{est} = 1 - \frac{tr\left[\langle \boldsymbol{d}^{a-b}(\boldsymbol{d}^{o-b})^{\mathrm{T}} \rangle\right]}{\rho\, tr[\mathbf{H}\mathbf{P}^{f}\mathbf{H}^{\mathrm{T}}]} \text{ and} \tag{29}$$

$$a^{est} = \frac{tr[\mathbf{H}\mathbf{P}^{\acute{a}}\mathbf{H}^{\mathrm{T}}] - tr[\langle \boldsymbol{d}^{a-b}(\boldsymbol{d}^{o-a})^{\mathrm{T}} \rangle]}{\rho\, tr[\mathbf{H}\mathbf{P}^{f}\mathbf{H}^{\mathrm{T}}]}, \tag{30}$$

respectively.

To estimate the diagonal components of $\mathbf{R}^{uc\_est} = diag\left(r_i^{uc\_est}\right)$ $(i = 1, \dots, p)$, a_i^{est} estimated from Eq. (27) is substituted into Eqs. (23) and (25). As a result, a single consistent equation is obtained as

$$r_i^{est} = \langle \boldsymbol{d}^{o-b}(\boldsymbol{d}^{o-b})^{\mathrm{T}} \rangle_{ii} - \frac{\langle \boldsymbol{d}^{a-b}(\boldsymbol{d}^{o-b})^{\mathrm{T}} \rangle_{ii}^{2}}{\rho(\mathbf{H}\mathbf{P}^{f}\mathbf{H}^{\mathrm{T}})_{ii}}. \tag{31}$$

In contrast, by substituting Eq. (28) into Eqs. (23) and (25), two equations to estimate $r_i^{uc\_est}$ are derived as

$$r_i^{uc\_est} = \langle \boldsymbol{d}^{o-b}(\boldsymbol{d}^{o-b})^{\mathrm{T}} \rangle_{ii} - \rho(\mathbf{H}\mathbf{P}^{f}\mathbf{H}^{\mathrm{T}})_{ii}\left[1 - \frac{(\mathbf{H}\mathbf{P}^{\acute{a}}\mathbf{H}^{\mathrm{T}})_{ii} - \langle \boldsymbol{d}^{a-b}(\boldsymbol{d}^{o-a})^{\mathrm{T}} \rangle_{ii}}{\rho(\mathbf{H}\mathbf{P}^{f}\mathbf{H}^{\mathrm{T}})_{ii}}\right]^{2} \text{ and} \tag{32}$$

$$r_i^{uc\_est} = \langle \boldsymbol{d}^{o-a}(\boldsymbol{d}^{o-b})^{\mathrm{T}} \rangle_{ii} + \left[\left(\mathbf{H}\acute{\mathbf{P}}^{a}\mathbf{H}^{\mathrm{T}}\right)_{ii} - \langle \boldsymbol{d}^{a-b}(\boldsymbol{d}^{o-a})^{\mathrm{T}} \rangle_{ii}\right]\left[1 - \frac{(\mathbf{H}\mathbf{P}^{\acute{a}}\mathbf{H}^{\mathrm{T}})_{ii} - \langle \boldsymbol{d}^{a-b}(\boldsymbol{d}^{o-a})^{\mathrm{T}} \rangle_{ii}}{\rho(\mathbf{H}\mathbf{P}^{f}\mathbf{H}^{\mathrm{T}})_{ii}}\right], \tag{33}$$

respectively. If a_i^{est} and $r_i^{uc\_est}$ are uniform (i.e., $\mathbf{A}^{est} = a^{est}\mathbf{I}^{p\times p}$ and $\mathbf{R}^{uc\_est} = r^{uc\_est}\mathbf{I}^{p\times p}$), Eqs. (31)–(33) reduce to

https://doi.org/10.5194/egusphere-2026-2653
Preprint. Discussion started: 11 June 2026

$$r^{uc\_est} = \frac{1}{p}\left\{ tr[\langle \boldsymbol{d}^{o-b}(\boldsymbol{d}^{o-b})^{\mathrm{T}}\rangle] - \frac{tr\left[\langle \boldsymbol{d}^{a-b}(\boldsymbol{d}^{o-b})^{\mathrm{T}}\rangle\right]^2}{\rho\, tr[\mathbf{H}\mathbf{P}^f\mathbf{H}^{\mathrm{T}}]} \right\}, \tag{34}$$

$$r^{uc\_est} = \frac{1}{p}\left\{ tr[\langle \boldsymbol{d}^{o-b}(\boldsymbol{d}^{o-b})^{\mathrm{T}}\rangle] - \rho\, tr[\mathbf{H}\mathbf{P}^f\mathbf{H}^{\mathrm{T}}]\left[1 - \frac{tr[\mathbf{H}\acute{\mathbf{P}}^a\mathbf{H}^{\mathrm{T}}] - tr[\langle \boldsymbol{d}^{a-b}(\boldsymbol{d}^{o-a})^{\mathrm{T}}\rangle]}{\rho\, tr[\mathbf{H}\mathbf{P}^f\mathbf{H}^{\mathrm{T}}]}\right]^2 \right\}, \text{ and} \tag{35}$$

$$r^{uc\_est} = \frac{1}{p}\left\{ tr[\langle \boldsymbol{d}^{o-a}(\boldsymbol{d}^{o-b})^{\mathrm{T}}\rangle] + \left[tr\left[\mathbf{H}\acute{\mathbf{P}}^a\mathbf{H}^{\mathrm{T}}\right] - tr[\langle \boldsymbol{d}^{a-b}(\boldsymbol{d}^{o-a})^{\mathrm{T}}\rangle]\right]\left[1 - \frac{tr[\mathbf{H}\acute{\mathbf{P}}^a\mathbf{H}^{\mathrm{T}}] - tr[\langle \boldsymbol{d}^{a-b}(\boldsymbol{d}^{o-a})^{\mathrm{T}}\rangle]}{\rho\, tr[\mathbf{H}\mathbf{P}^f\mathbf{H}^{\mathrm{T}}]}\right] \right\}, \tag{36}$$

respectively.

In summary, $\mathbf{A}^{est} = diag(a_i^{est})$ and $\mathbf{R}^{uc\_est} = diag\left(r_i^{uc\_est}\right)$ can be estimated from three combinations: Eqs. (27) and (31); Eqs. (28) and (32); and Eqs. (28) and (33). In the uniform parameter case (i.e., $\mathbf{A}^{est} = a^{est}\mathbf{I}^{p\times p}$ and $\mathbf{R}^{uc\_est} = r^{uc\_est}\mathbf{I}^{p\times p}$), Eqs. (29) and (34), Eqs. (30) and (35), and Eqs. (30) and (36) can be alternatively used.

3 Experimental setting

This study used the Lorenz-96 model (Lorenz and Emanuel, 1998) with 40 variables and a cyclic boundary condition:

$$\frac{dx_i}{dt} = (x_{i+1} - x_{i-2})x_{i-1} - x_i + F\,, \tag{37}$$

where $i = 1, 2, \ldots, 40$ is the index of the model grid point, t is time, and $F = 8.0$ is an external forcing parameter. $\Delta t = 0.05$ model timestep corresponds to 6 hours if we consider the typical error-doubling time for the synoptic weather (Lorenz and Emanuel, 1998). The fourth-order Runge–Kutta scheme with $\Delta t = 0.01$ is applied. These experimental settings follow previous studies (e.g., OKM25).

In this study, we performed perfect-model twin experiments without system noise or model errors. An 11-year nature run was conducted after a 1-year spin-up initialized from a standard Gaussian random noise. As discussed in Sect. 1, some systems assimilate optimal interpolated analysis data, in which background and observation error covariance matrices are generally fixed in space and time. Consequently, it is reasonable to assume $\mathbf{A} = a\mathbf{I}^{40\times 40}$ and $\mathbf{H} = \mathbf{I}^{40\times 40}$. Observations were generated every 6 hours at all model grid points by adding $\boldsymbol{\epsilon}^o = \mathbf{H}\boldsymbol{\epsilon}^f + \boldsymbol{\eta} = a\boldsymbol{\epsilon}^f + \boldsymbol{\eta}$ [Eq. (1)] to $\boldsymbol{x}^{true}$ from the nature run. Here, $\boldsymbol{\epsilon}^f = \overline{\boldsymbol{x}^f} - \boldsymbol{x}^{true}$ was calculated online, and we set $a = -1.0, -0.9, \ldots, 0.9$ and $\boldsymbol{\eta}\sim N(\mathbf{0}, \mathbf{R}^{uc} = \mathbf{I}^{40\times 40})$. $a > 0$ (i.e., positive cross-correlation between the forecast and observation errors) arises when the forecast errors contaminate the observation error, whereas $a < 0$ (i.e., negative cross-correlation) would be unrealistic in practice. Nevertheless, $a < 0$ is included in this study for theoretical completeness.

After a 1-year ensemble spin-up initialized from the different Gaussian random noises with the nature run, we conducted three types of sensitivity experiments for 11 years: (i) standard ETKF experiments, (ii) ETKFCC experiments

https://doi.org/10.5194/egusphere-2026-2653
Preprint. Discussion started: 11 June 2026

with the estimated parameters, and (iii) ETKFCC experiments with the prescribed true parameters. The standard ETKF experiments used Eqs. (11)–(13) derived under the assumption of no cross-correlation, but assimilated correlated observations. Since $\mathbf{R} \cong \rho\mathbf{A}\mathbf{H}\mathbf{P}^f\mathbf{H}^{\mathrm{T}}\mathbf{A}^{\mathrm{T}} + \mathbf{R}^{uc}$ depends on $\mathbf{P}^f$, not only $\rho = 1.00, 1.01, \ldots, 1.1, 1.2, \ldots, 2.0, 3.0, \ldots, 5.0$ but also $\mathbf{R} = 1.0, 1.1, \cdots, 2.0, 3.0, \cdots, 10.0 \times \mathbf{I}^{40\times40}$ were tuned. By substituting $\widehat{\boldsymbol{\sigma}^f}$, $\widehat{\boldsymbol{\sigma}^a}$, $\boldsymbol{d}^{o-b}$, $\boldsymbol{d}^{o-a}$, and $\boldsymbol{d}^{a-b}$ from the standard ETKF experiments into Eqs. (29), (30), and (34)–(36), we estimated three combinations of parameters a^{est} and r^{uc_est}. Substituting the estimated and prescribed true parameters into the ETKFCC formulations [Eqs. (8)–(10)], we conducted two kinds of ETKFCC experiments, tuning $\rho = 1.00, 1.01, \ldots, 1.10$. We note that filter divergence occurs in both the ETKF and ETKFCC experiments when $\rho < 1$, regardless of the presence or absence of the cross-correlation. Covariance localization in observation space can be applied to $\mathbf{R}$ and $\mathbf{R}^{uc}$ in the ETKF and ETKFCC, respectively. However, to avoid introducing an additional tuning parameter, covariance localization is not applied, as a sufficiently large ensemble size of 40 members is used for the 40-dimensional system.

Using $\boldsymbol{\epsilon}^f = \overline{\boldsymbol{x}^f} - \boldsymbol{x}^{true}$, $\boldsymbol{\epsilon}^a = \overline{\boldsymbol{x}^a} - \boldsymbol{x}^{true}$ and $\boldsymbol{\epsilon}^o$ at each analysis timestep, we calculated spatiotemporally averaged forecast and analysis ensemble spreads over the entire domain and the last 10 years, as well as the corresponding forecast, analysis, and observational root-mean-square errors (RMSEs), and then compared them among the three experiments. Since observational RMSEs are different among the sensitivity experiments, we defined $RMSE\ ratio = \frac{analysis\ RMSE}{observational\ RMSE}$, and $improvement\ ratio\ (\%) = 100 \times \left(1 - \frac{RMSE\ ratio\ in\ ETKFCC}{RMSE\ ratio\ in\ ETKF}\right)$. We applied the bootstrap method to the spatially averaged RMSE ratio differences among the three experiments at a 99% confidence level, resampling 100,000 times from the last 10-year experiments. We also estimated the cross-correlation coefficients between the forecast and observation errors for each model grid point and then spatiotemporally averaged them over the entire domain and analysis period. In this study, we defined filter divergence as the spatiotemporally averaged analysis RMSE being larger than the corresponding observational RMSE.

4 Result

4.1 Parameter estimation

Figure 1 shows the spatiotemporally averaged analysis RMSEs in the standard ETKF experiments. The results show lower accuracy for more positive a^{true}, and vice versa for negative a^{true}, as consistent with OKM25. For large positive a^{true}, large inflation parameters are required to achieve the best analysis accuracy.

https://doi.org/10.5194/egusphere-2026-2653
Preprint. Discussion started: 11 June 2026

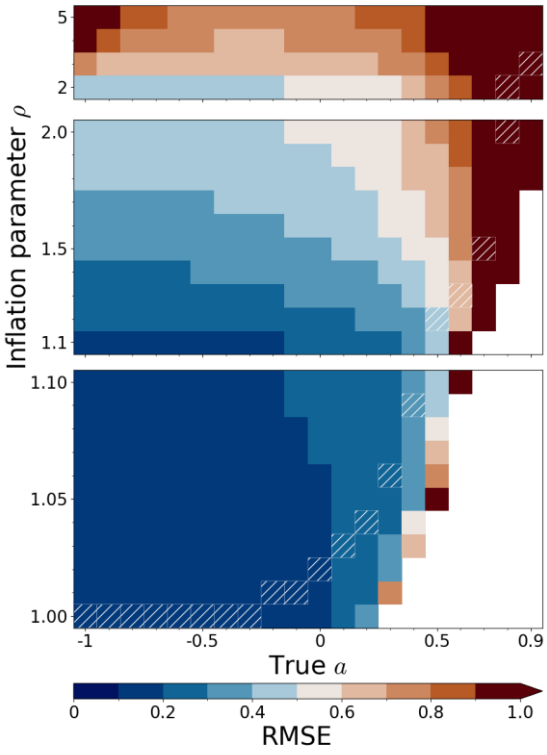

Figure 1: Spatiotemporally averaged analysis RMSEs in the standard ETKF experiments. White hatches indicate the minimum analysis RMSEs for each a^{true}, and white color indicates filter divergence.

Using the results from the optimal ETKF experiments, we estimated a^{est} and r^{uc_est} (Fig. 2). a^{est} from both Eqs. (29) and (30) are well estimated for positive a^{true}, while they deviate substantially from a^{true} for negative a^{true} (Fig. 2a). However, this discrepancy is not critical because observations are unlikely to have negative a (i.e., negative cross-correlation between the forecast and observation errors) in practice as discussed in Sect. 3. For positive a^{true}, a^{est} from Eq. (29) with $\langle \boldsymbol{d}^{a-b}(\boldsymbol{d}^{o-b})^{\mathrm{T}} \rangle$ is closer to a^{true} than that from Eq. (30) with $\langle \boldsymbol{d}^{o-a}(\boldsymbol{d}^{o-b})^{\mathrm{T}} \rangle$.

From Eqs. (34)–(36), we estimated three types of r^{uc_est} (Fig. 2b). Among these, r^{uc_est} from Eq. (34) is the closest to r^{uc_true}, while r^{uc_est} from Eqs. (35) and (36) are exceedingly far from r^{uc_true} for $a^{true} \geq 0.7$.

According to Eq. (29), the accuracy of a^{est} depends on that of the forecast ensemble spread. When $a^{true} < 0$ and $0.7 \leq a^{true} \leq 0.9$, $a^{est} > a^{true}$ because the forecast ensemble spread is overestimated (blue line in Fig. 2c). Conversely, for $0.1 \leq a^{true} \leq 0.5$, the spread is underestimated, resulting in $a^{est} < a^{true}$. The accuracy of a^{est} in Eq. (30) is influenced by both analysis and forecast ensemble spreads. From Eq. (30) in scalar form,

https://doi.org/10.5194/egusphere-2026-2653
Preprint. Discussion started: 11 June 2026

$$a^{est} = \left(\widehat{\sigma^a}^2 - \langle d^{a-b} d^{o-a} \rangle\right) / \left(\rho \widehat{\sigma^f}^2\right), \text{ and} \quad (38)$$

$$a^{true} = (MSE^a - \langle d^{a-b} d^{o-a} \rangle) / MSE^f, \quad (39)$$

where MSE^f and MSE^a are forecast and analysis mean square errors (MSEs), respectively. Let $MSE^f + \delta\widehat{\sigma^f}^2 = \rho\widehat{\sigma^f}^2$ and $MSE^a + \delta\widehat{\sigma^a}^2 = \widehat{\sigma^a}^2$, where $\delta\widehat{\sigma^f}^2$ and $\delta\widehat{\sigma^a}^2$ denote errors in the forecast and analysis ensemble spreads relative to the corresponding MSEs. The estimation error $\delta a^{est} \equiv a^{est} - a^{true}$ is then given by

$$\delta a^{est} = \frac{MSE^f \delta\widehat{\sigma^a}^2 - \left(MSE^a - \langle d^{a-b} d^{o-a} \rangle\right) \delta\widehat{\sigma^f}^2}{MSE^f \left(MSE^f + \delta\widehat{\sigma^f}^2\right)} = \frac{\delta\widehat{\sigma^a}^2 - a^{true} \delta\widehat{\sigma^f}^2}{MSE^f + \delta\widehat{\sigma^f}^2}. \quad (40)$$

For negative a^{true}, both forecast and analysis ensemble spreads are overestimated (blue and red lines in Fig. 2c, respectively), resulting in $a^{est} > a^{true}$. The underestimation of the analysis ensemble spread for $0.1 \leq a^{true} \leq 0.7$ and the overestimation of the forecast ensemble spread for $0.8 \leq a^{true} \leq 0.9$ are the primary causes of $a^{est} < a^{true}$. Thus, the accuracy of a^{est} is determined by the accuracy of both forecast and analysis ensemble spreads.

https://doi.org/10.5194/egusphere-2026-2653
Preprint. Discussion started: 11 June 2026

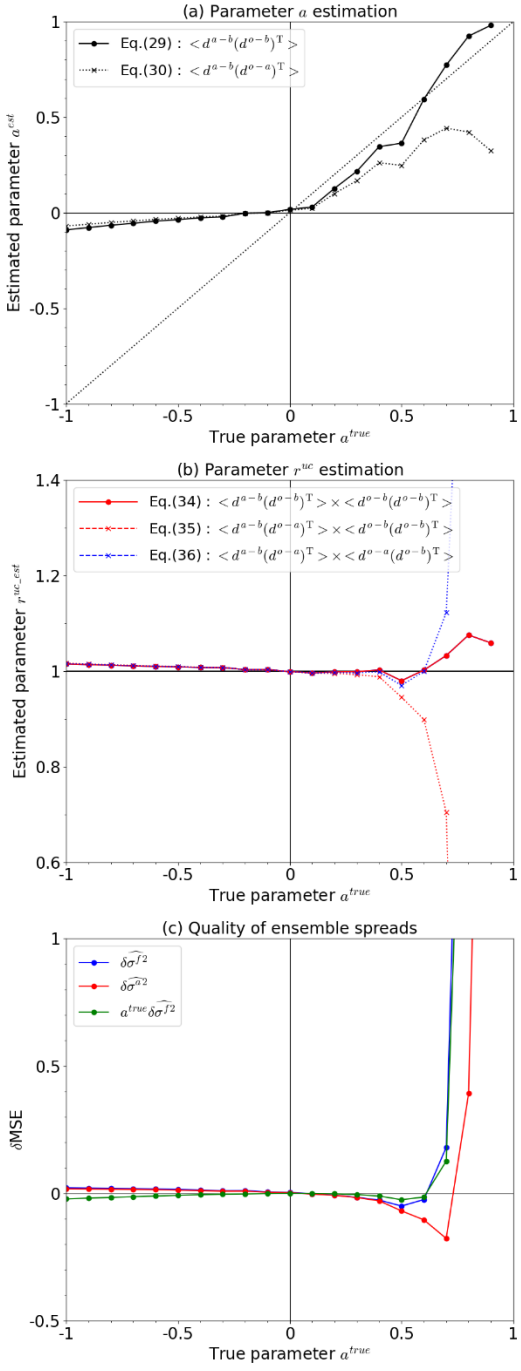

230 **Figure 2:** (a) a^{est} and (b) r^{uc_est} estimated from standard ETKF experiments optimally tuned for each a^{true}. Solid and dotted lines in (a) correspond to a^{est} from Eqs. (29) and (30) with $\langle \boldsymbol{d}^{a-b}(\boldsymbol{d}^{o-b})^{\mathrm{T}} \rangle$ and $\langle \boldsymbol{d}^{o-a}(\boldsymbol{d}^{o-b})^{\mathrm{T}} \rangle$, respectively. In (b), the red solid, red dotted, and blue dotted lines represent r^{uc_est} estimated from Eqs. (34), (35), and (36), respectively. (c)

https://doi.org/10.5194/egusphere-2026-2653
Preprint. Discussion started: 11 June 2026

Differences of the spatiotemporally averaged forecast and analysis ensemble spreads with the corresponding forecast and analysis MSEs: $\delta\widehat{\sigma^f}^2 = \rho\widehat{\sigma^f}^2 - MSE^f$ and $\delta\widehat{\sigma^a}^2 = \widehat{\sigma^a}^2 - MSE^a$ (blue and red lines, respectively). In (c), green line indicates $a^{true}\delta\widehat{\sigma^f}^2$, which is shown for direct comparison with $\delta\widehat{\sigma^a}^2$ in Eq. (38).

Both a^{est} and the forecast ensemble spread appear in the first term on the right-hand side of Eq. (23), which leads to Eq. (34) for estimating r^{uc_est}. Since the overestimation and underestimation of a^{est} from Eq. (29) arise from the corresponding errors in the forecast ensemble spread, respectively, these errors tend to offset each other in Eq. (34), resulting in accurate r^{uc_est}. In contrast, such error cancellation does not occur in the estimation of r^{uc_est} using Eqs. (35) and (36).

Therefore, the estimated parameters a^{est} and r^{uc_est} from Eqs. (29) and (34), respectively, are the most accurate and are exclusively used in the ETKFCC experiments with the estimated parameters.

4.2 Sensitivity experiments

We conducted the ETKFCC experiments using a^{est} and r^{uc_est} from Eqs. (29) and (34), respectively (Fig. 3). The results show lower accuracy and larger ensemble spread for more positive a^{true}, and vice versa for negative a^{true} (Fig. 3a–c). The cross-correlation coefficients between the forecast and observation errors are positive and negative for positive and negative a^{true}, respectively, theoretically consistent as Eq. (2) of OKM25 (Fig. 3d). The optimal inflation parameters range from 1.00 to 1.08 and do not show the exceedingly large inflations seen in the standard ETKF experiments (cf. Fig. 1). For $a^{true} = 0.9$, filter divergence occurs in all the ETKFCC experiments, likely because a^{est} estimated from Eq. (29) is nearly 1.0, leading to $\acute{\mathbf{K}} \cong \mathbf{0}$ and $\boldsymbol{x}^a \cong \boldsymbol{x}^f$.

https://doi.org/10.5194/egusphere-2026-2653
Preprint. Discussion started: 11 June 2026

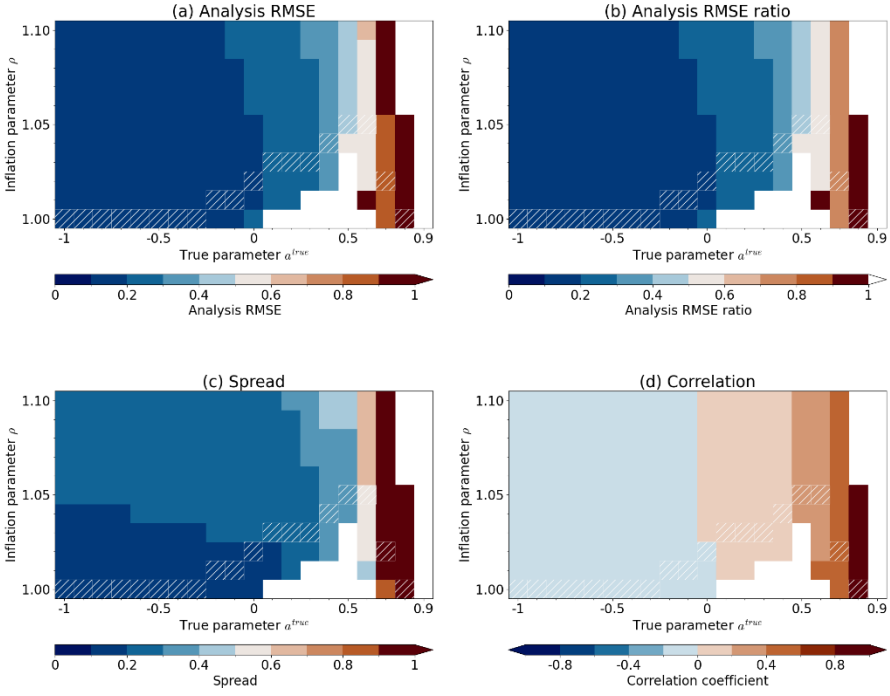

Figure 3: Spatiotemporally averaged (a) analysis RMSEs, (b) RMSE ratios, (c) analysis ensemble spreads, and (d) cross-correlation coefficients between the forecast and observation errors in the ETKFCC experiments with estimated parameters a^{est} and r^{uc_est}. White hatches indicate the minimum analysis RMSEs for each a^{true}, and white color indicates filter divergence.

The optimal ETKFCC with the estimated parameters was compared with the standard ETKF and the ETKFCC with the prescribed true parameters (Fig. 4). Although the RMSE ratios in the ETKFCC with the estimated parameters are comparable to those in the standard ETKF for $a^{true} \leq 0.4$, they are significantly and 5% more accurate than the standard ETKF for $0.5 \leq a^{true} \leq 0.7$ (Fig. 4a). From a line plot in which with the cross-correlation coefficient between the forecast and observation errors is shown on the horizontal axis (Fig. 4b), the ETKFCC with the estimated parameters is more accurate than the standard ETKF when the cross-correlation coefficients are between 0.2 and 0.7. Therefore, the ETKFCC with the estimated parameters outperforms the standard ETKF but does not outperform the ETKFCC with the prescribed true parameters.

https://doi.org/10.5194/egusphere-2026-2653
Preprint. Discussion started: 11 June 2026

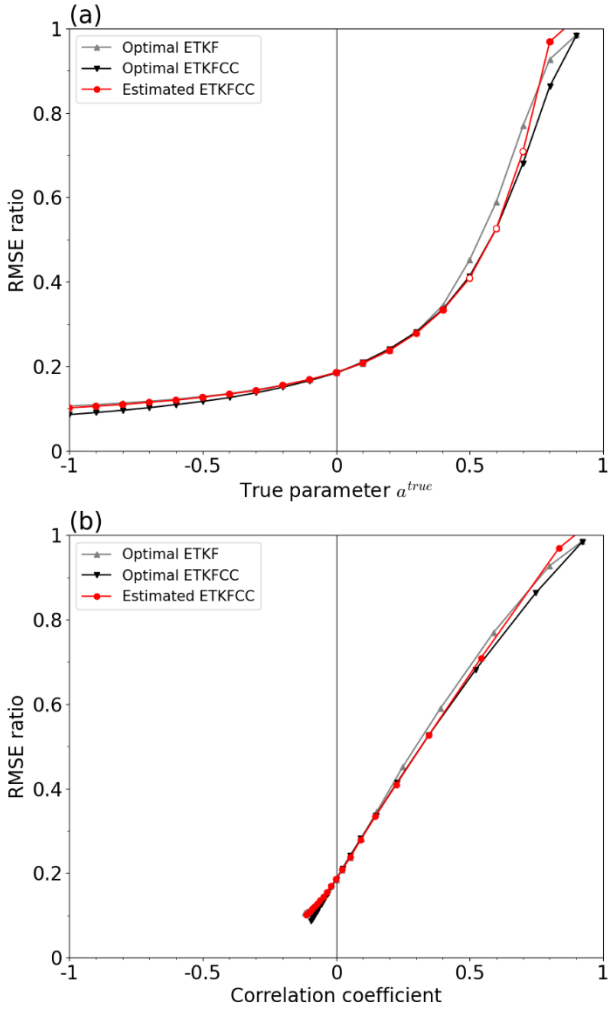

Figure 4: Spatiotemporally averaged analysis RMSE ratios of the optimal standard ETKF experiment (gray) and the ETKFCC experiments with the estimated (red) and prescribed true (black) parameters, relative to (a) a^{true} and (b) the cross-correlation coefficients between the forecast and observation errors.

5 Discussion

It is difficult to optimally tune parameters, such as covariance inflation and observation errors, in practice because the huge computational costs might be required. In this section, we estimated a^{est} and r^{uc_est} from all the standard ETKF experiments, intentionally including suboptimal experiments. Although the standard ETKF experiments have two tuning parameters (ρ and **R**), we show the results where **R** is optimally tuned but ρ is not, for clarity. Figure 5 shows the differences

https://doi.org/10.5194/egusphere-2026-2653
Preprint. Discussion started: 11 June 2026

of a^{est} and r^{uc_est} estimated from the optimally **R** tuned standard ETKF experiments with the prescribed true parameters. When ρ approaches its optimal values (i.e., white hatches), a^{est} is close to a^{true} for positive a^{true}, while a^{est} is not estimated accurately for negative a^{true} (Fig. 5a). As ρ approaches its optimal values, r^{uc_est} approaches r^{uc_true}, but compared with a^{est}, r^{uc_est} is less sensitive to the tuning (Fig. 5b).

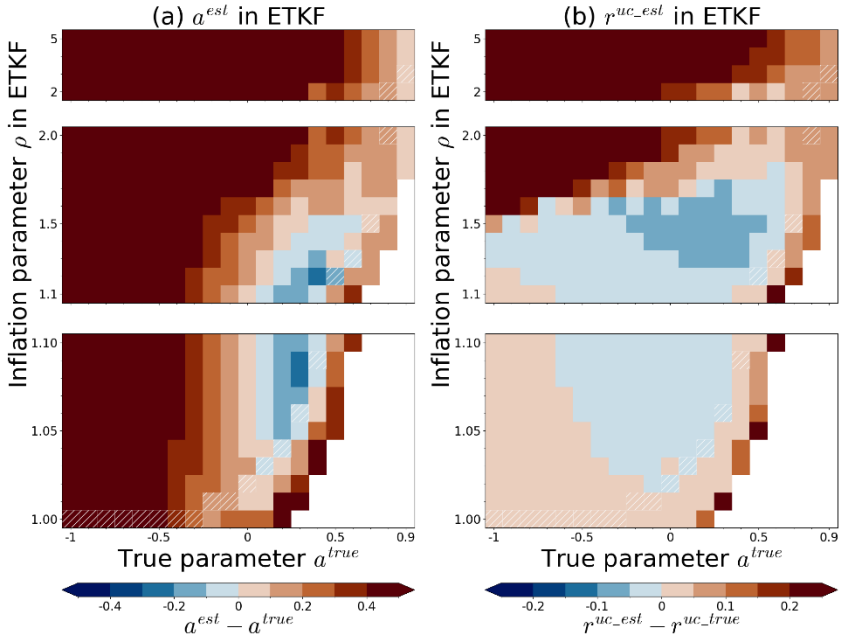

Figure 5: The differences of (a) a^{est} and (b) r^{uc_est} estimated from the standard ETKF experiments using optimal **R** with the prescribed true parameters a^{true} and r^{uc_true}. White hatches indicate the standard ETKF experiments with the minimum analysis RMSE for each a^{true}, and white color indicates filter divergence.

Applying a^{est} and r^{uc_est} estimated from all the standard ETKF experiments to the ETKFCC [Eqs. (8)–(10)], we conducted the ETKFCC experiments by tuning ρ. Figure 6b shows the analysis RMSE ratios of the optimally tuned ETKFCC experiments, and Fig. 6c indicates the RMSE ratio differences between the ETKFCC and standard ETKF experiments (i.e., Fig. 6b minus Fig. 6a). The RMSE ratios are smaller in the ETKFCC experiments than in the standard ETKF experiments in most parameter settings (Fig. 6c), and therefore the results suggest that the offline parameter estimation approach proposed in this study can improve analysis accuracy even if tuning parameters are suboptimal.

https://doi.org/10.5194/egusphere-2026-2653
Preprint. Discussion started: 11 June 2026

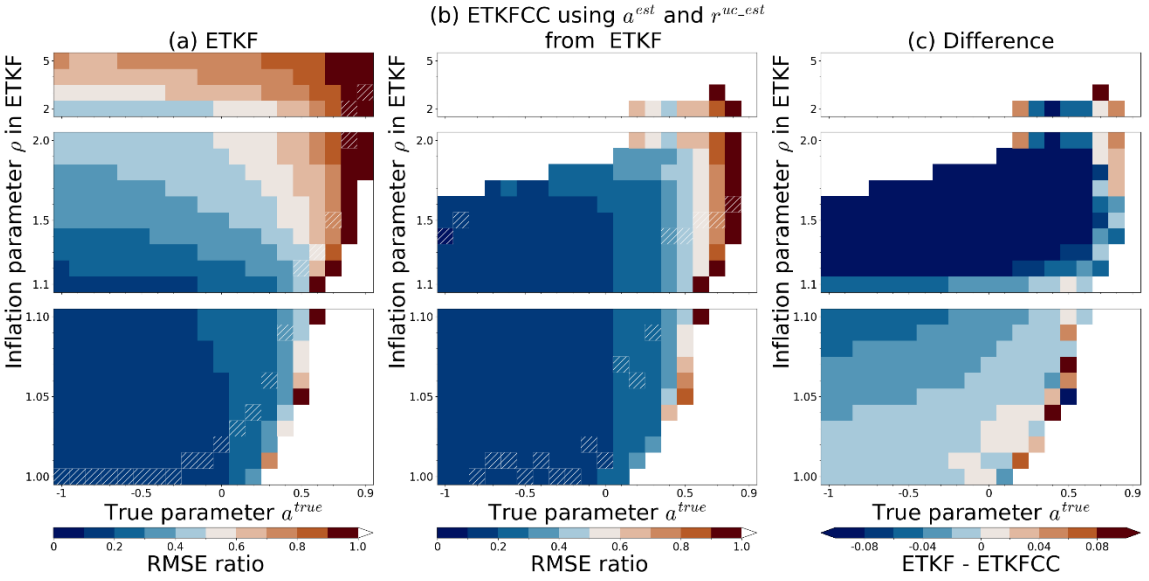

Figure 6: Analysis RMSE ratios in (a) the standard ETKF and (b) the optimally tuned ETKFCC experiments with a^{est} and r^{uc_est} estimated from the standard ETKF experiments shown in (a). (c) Difference between (b) and (a). In (b) and (c), the vertical axes are inflation parameters used in (a) the standard ETKF experiments. In (a) and (b), white hatches indicate the ETKF and ETKFCC experiments that are optimally tuned for each a^{true}, respectively. In (c), red and blue colors represent higher accuracy in the (a) standard ETKF and (b) ETKFCC experiments, respectively. White color indicates filter divergence.

6 Summary

In this study, we extended the innovation statistics of Desroziers et al. (2005) to include the cross-correlations between the observation and forecast errors and proposed an offline approach to estimate the cross-correlation parameters a and r^{uc}. To investigate the feasibility of the proposed method, we performed a series of the Lorenz-96 perfect-model twin experiments. First, we conducted standard EnKF experiments assimilating observations whose errors were correlated with the forecast errors. We applied our proposed approach to the optimal results of the standard ETKF experiments and estimated the cross-correlation parameters. Next, we performed ETKFCC experiments using the estimated parameters and compared with the standard ETKF and the ETKFCC using the prescribed true parameters. The results showed that the innovation statistics combining $\langle \boldsymbol{d}^{a-b}(\boldsymbol{d}^{o-b})^{\mathrm{T}} \rangle$ [Eq. (29)] with either $\langle \boldsymbol{d}^{o-b}(\boldsymbol{d}^{o-b})^{\mathrm{T}} \rangle$ or $\langle \boldsymbol{d}^{o-a}(\boldsymbol{d}^{o-b})^{\mathrm{T}} \rangle$ [Eq. (34)] well estimated both a and r^{uc} for the positive cross-correlations between the forecast and observation errors (i.e., positive a^{true}) (Fig. 2). In contrast, all innovation statistics failed to estimate a for the negative cross-correlations (i.e., negative a^{true});

https://doi.org/10.5194/egusphere-2026-2653
Preprint. Discussion started: 11 June 2026

however, this is not a crucial issue because observations negatively correlated with the forecast errors would not exist in practice.

The validation results demonstrated that in the standard ETKF experiments, exceedingly large inflations were required to achieve optimal accuracy for $a^{true} \geq 0.5$ (Fig. 1), whereas in the ETKFCC experiments using the estimated parameters, such inflations were not necessary (Fig. 3). When the cross-correlation coefficient between the forecast and observation errors was 0.2–0.7 (i.e., $a^{true} = 0.5 - 0.7$), the optimal ETKFCC with the estimated parameters was significantly more accurate than the optimal standard ETKF, but did not surpass the optimal ETKFCC experiment with the prescribed true parameters (Fig. 4). For the other cross-correlation coefficients, the optimal ETKFCC with the estimated parameters showed comparable accuracy to the optimal standard ETKFCC.

Since in practice it would require high computational costs to optimize the tuning parameters of the standard ETKF, we also investigated the ETKFCC that uses the cross-correlation parameters estimated from suboptimal ETKF experiments. We obtained robust results, so that the ETKFCC with the suboptimally estimated parameters outperformed the standard ETKF (Fig. 6).

In this study, we assumed that optimal interpolation analysis data were assimilated and that the estimated parameters were spatially uniform (i.e., $\mathbf{A} = a\mathbf{I}^{p\times p}$ and $\mathbf{R}^{uc} = r^{uc}\mathbf{I}^{p\times p}$). If multiple types of observations are assimilated, we need to use innovation statistics with non-uniform parameters [Eqs. (27), (28), and (31)–(33)] or estimate parameters serially for each observation type. In our future research, we plan to apply the ETKFCC to practical data assimilation systems.

Appendices

Appendix A: Notations

Table A1: Notations for scalars

Symbol	Definition
a	Scalar parameter for correlated observation errors
r	Scalar parameter for correlated observation errors
F	Forcing parameter in Lorenz-96
m	Ensemble size
n	Model dimension
p	Observation dimension

https://doi.org/10.5194/egusphere-2026-2653
Preprint. Discussion started: 11 June 2026

t	Time
Δt	Model timestep
x	State variable
ϵ	Error
σ	Error standard deviation
ρ	Multiplicative inflation parameter ($\rho \geq 1$)

Table A2: Notations for superscripts

Symbol	Definition
$(\cdot)^a$	Analysis
$(\cdot)^f$	Forecast
$(\cdot)^{(i)}$	ith ensemble member ($i = 1,2, \ldots, m$)
$(\cdot)^o$	Observation
$(\cdot)^{true}$	True
$(\cdot)^{est}$	Estimation
$(\cdot)^{\mathrm{T}}$	Transpose
$(\cdot)^{uc}$	Uncorrelated with the forecast errors
$(\cdot)^{-1}$	Inverse
$\acute{(\cdot)}$	Including the cross-correlation between the forecast and observation errors
$\overline{(\cdot)}$	Ensemble mean
$\widehat{(\cdot)}$	Ensemble-based sample estimate

https://doi.org/10.5194/egusphere-2026-2653
Preprint. Discussion started: 11 June 2026

335 **Table A3:** Notations for subscripts

Symbol	Definition
$(\cdot)_i$	*i*th element for vectors, *i*th diagonal element for matrices
$(\cdot)_{ij}$	Element for matrix in *i*th row and *j*th column

Table A4: Notations for vectors

Symbol	Definition	Dimension
$\boldsymbol{x}$	State vector	$\mathbb{R}^n$
$\boldsymbol{y}$	Observation	$\mathbb{R}^p$
$\boldsymbol{\epsilon}$	Error	$\mathbb{R}^n$ for $\boldsymbol{\epsilon}^f$ and $\boldsymbol{\epsilon}^a$ $\mathbb{R}^p$ for $\boldsymbol{\epsilon}^o$
$\boldsymbol{\eta}$	Gaussian random noise: $\boldsymbol{\eta}\sim N(\mathbf{0}, \mathbf{R}^{uc})$	$\mathbb{R}^p$
$\boldsymbol{d}$	Difference among state vector and observation in observation space	$\mathbb{R}^p$

Table A5: Notations for matrices

Symbol	Definition	Dimension
$\mathbf{A}$	$\mathbf{A} = diag(a_i)$	$\mathbb{R}^{p\times p}$
$\mathbf{C}$	Covariance matrix between the forecast and observation errors: $\mathbf{C} = \langle \boldsymbol{\epsilon}^f (\boldsymbol{\epsilon}^o)^{\mathrm{T}} \rangle$	$\mathbb{R}^{n\times p}$
$\mathbf{H}$	Linear observation operator	$\mathbb{R}^{n\times p}$
$\mathbf{I}^{m\times m}$	m-by-m identity matrix	$\mathbb{R}^{m\times m}$
$\mathbf{I}^{n\times n}$	n-by-n identity matrix	$\mathbb{R}^{n\times n}$
$\mathbf{I}^{p\times p}$	p-by-p identity matrix	$\mathbb{R}^{p\times p}$

https://doi.org/10.5194/egusphere-2026-2653
Preprint. Discussion started: 11 June 2026

$\mathbf{K}$	Gain matrix	$\mathbb{R}^{n\times p}$
$\mathbf{P}$	Error covariance matrix: $\mathbf{P} = \langle \boldsymbol{\epsilon}\boldsymbol{\epsilon}^{\mathrm{T}} \rangle$	$\mathbb{R}^{n\times n}$
$\widetilde{\mathbf{P}}^{a}$	Error covariance matrix in ensemble space: $\widetilde{\mathbf{P}}^{a} = (m-1)^{-1}\mathbf{W}\mathbf{W}^{\mathrm{T}}$	$\mathbb{R}^{m\times m}$
$\mathbf{R}$	Observation error covariance matrix $\mathbf{R} = \langle \boldsymbol{\epsilon}^{o}(\boldsymbol{\epsilon}^{o})^{\mathrm{T}} \rangle$	$\mathbb{R}^{p\times p}$
$\mathbf{R}^{uc}$	Error covariance matrix of $\boldsymbol{\eta}$: $\mathbf{R}^{uc} = \langle \boldsymbol{\eta}\boldsymbol{\eta}^{\mathrm{T}} \rangle$	$\mathbb{R}^{p\times p}$
$\delta\mathbf{X}$	Ensemble perturbation matrix in model space: $\delta\mathbf{X} = (\boldsymbol{x}^{(1)} - \overline{\boldsymbol{x}}, \boldsymbol{x}^{(2)} - \overline{\boldsymbol{x}}, \dots, \boldsymbol{x}^{(m)} - \overline{\boldsymbol{x}})$	$\mathbb{R}^{n\times m}$
$\delta\mathbf{Y}$	Ensemble perturbation matrix in observation space: $\delta\mathbf{Y} = \mathbf{H}\delta\mathbf{X}$	$\mathbb{R}^{p\times m}$
$\mathbf{W}$	Transform matrix	$\mathbb{R}^{m\times m}$

340

Table A6: Notations for operators and normal distributions

Symbol	Definition
$H(\cdot)$	Non-linear observation operator
$M(\cdot)$	Model temporal evolution operator
$tr[\cdot]$	Trace
$\langle \cdot \rangle$	Expected value
$N(\boldsymbol{\mu}, \boldsymbol{\Sigma})$	Normal distribution in multiple dimensions with mean $\boldsymbol{\mu}$ and covariance matrix $\boldsymbol{\Sigma}$
$\delta(\cdot)$	Difference from the reference
δ_{ij}	Kronecker delta

https://doi.org/10.5194/egusphere-2026-2653
Preprint. Discussion started: 11 June 2026

Appendix B: Detailed formulation of innovation statistics with the cross-correlation between the forecast and observation errors

Using Eq. (5), $\acute{\mathbf{K}}$ [Eq. (4)] is represented as a different form as follows:

$$\acute{\mathbf{K}}(\rho\mathbf{H}\mathbf{P}^f\mathbf{H}^{\mathrm{T}} - \mathbf{H}\mathbf{C} - \mathbf{C}^{\mathrm{T}}\mathbf{H}^{\mathrm{T}} + \mathbf{R}) = \rho\mathbf{P}^f\mathbf{H}^{\mathrm{T}} - \mathbf{C}\ , \text{and therefore,} \tag{B1}$$

$$\begin{aligned}\acute{\mathbf{K}}(\mathbf{R} - \mathbf{H}\mathbf{C}) &= -\rho\acute{\mathbf{K}}\mathbf{H}\mathbf{P}^f\mathbf{H}^{\mathrm{T}} + \acute{\mathbf{K}}\mathbf{C}^{\mathrm{T}}\mathbf{H}^{\mathrm{T}} + \rho\mathbf{P}^f\mathbf{H}^{\mathrm{T}} - \mathbf{C} \\ &= \left[\rho\left(\mathbf{I}^{n\times n} - \acute{\mathbf{K}}\mathbf{H}\right)\mathbf{P}^f + \acute{\mathbf{K}}\mathbf{C}^{\mathrm{T}}\right]\mathbf{H}^{\mathrm{T}} - \mathbf{C} \\ &= \acute{\mathbf{P}}^a\mathbf{H}^{\mathrm{T}} - \mathbf{C}\ . \end{aligned} \tag{B2}$$

From Eq. (5),

$$\acute{\mathbf{K}}(\rho\mathbf{H}\mathbf{P}^f - \mathbf{C}^{\mathrm{T}}) = \rho\mathbf{P}^f - \acute{\mathbf{P}}^a\ . \tag{B3}$$

Therefore, using Eqs. (14)–(16) and (B2)–(B3), innovation statistics with the cross-correlation is derived as

$$\begin{aligned}\langle \boldsymbol{d}^{o-b}(\boldsymbol{d}^{o-b})^{\mathrm{T}}\rangle &= \langle\{\boldsymbol{\epsilon}^o - H(\boldsymbol{\epsilon}^f)\}\{\boldsymbol{\epsilon}^o - H(\boldsymbol{\epsilon}^f)\}^T\rangle \\ &\cong \mathbf{R} - \mathbf{H}\mathbf{C} - \mathbf{C}^{\mathrm{T}}\mathbf{H}^{\mathrm{T}} + \rho\mathbf{H}\mathbf{P}^f\mathbf{H}^{\mathrm{T}}\ , \end{aligned} \tag{B4}$$

$$\begin{aligned}\langle \boldsymbol{d}^{a-b}(\boldsymbol{d}^{o-b})^{\mathrm{T}}\rangle &= \mathbf{H}\acute{\mathbf{K}}\langle \boldsymbol{d}^{o-b}(\boldsymbol{d}^{o-b})^{\mathrm{T}}\rangle \\ &= \mathbf{H}\acute{\mathbf{K}}(\mathbf{R} - \mathbf{H}\mathbf{C}) + \mathbf{H}\acute{\mathbf{K}}(\rho\mathbf{H}\mathbf{P}^f - \mathbf{C}^{\mathrm{T}})\mathbf{H}^{\mathrm{T}} \\ &= \mathbf{H}\left(\acute{\mathbf{P}}^a\mathbf{H}^{\mathrm{T}} - \mathbf{C}\right) + \mathbf{H}\left(\rho\mathbf{P}^f - \acute{\mathbf{P}}^a\right)\mathbf{H}^{\mathrm{T}} \\ &= -\mathbf{H}\mathbf{C} + \rho\mathbf{H}\mathbf{P}^f\mathbf{H}^{\mathrm{T}}\ , \end{aligned} \tag{B5}$$

$$\begin{aligned}\langle \boldsymbol{d}^{o-a}(\boldsymbol{d}^{o-b})^{\mathrm{T}}\rangle &= \left(\mathbf{I}^{p\times p} - \mathbf{H}\acute{\mathbf{K}}\right)\langle \boldsymbol{d}^{o-b}(\boldsymbol{d}^{o-b})^{\mathrm{T}}\rangle \\ &= \langle \boldsymbol{d}^{o-b}(\boldsymbol{d}^{o-b})^{\mathrm{T}}\rangle - \langle \boldsymbol{d}^{a-b}(\boldsymbol{d}^{o-b})^{\mathrm{T}}\rangle \\ &= \mathbf{R} - \mathbf{C}^{\mathrm{T}}\mathbf{H}^{\mathrm{T}}\ , \text{and} \end{aligned} \tag{B6}$$

$$\begin{aligned}\langle \boldsymbol{d}^{a-b}(\boldsymbol{d}^{o-a})^{\mathrm{T}}\rangle &= \mathbf{H}\acute{\mathbf{K}}\langle \boldsymbol{d}^{o-b}(\boldsymbol{d}^{o-b})^{\mathrm{T}}\rangle\left(\mathbf{I}^{p\times p} - \mathbf{H}\acute{\mathbf{K}}\right)^{\mathrm{T}} \\ &= \mathbf{H}\acute{\mathbf{K}}\langle \boldsymbol{d}^{o-a}(\boldsymbol{d}^{o-b})^{\mathrm{T}}\rangle^{\mathrm{T}} \\ &= \mathbf{H}\acute{\mathbf{K}}(\mathbf{R} - \mathbf{H}\mathbf{C}) \\ &= \mathbf{H}\acute{\mathbf{P}}^a\mathbf{H}^{\mathrm{T}} - \mathbf{H}\mathbf{C}\ . \end{aligned} \tag{B7}$$

From $\boldsymbol{\epsilon}^o = \mathbf{A}H(\boldsymbol{\epsilon}^f) + \boldsymbol{\eta}$ [Eq. (1)] and $\langle \boldsymbol{\epsilon}^f\boldsymbol{\eta}^{\mathrm{T}}\rangle = \mathbf{O}$ [Eq. (2)], through the linearization of the observation operator, $\mathbf{R}$ and $\mathbf{C}$ are represented as

https://doi.org/10.5194/egusphere-2026-2653
Preprint. Discussion started: 11 June 2026

$$\mathbf{R} = \langle \boldsymbol{\epsilon}^o (\boldsymbol{\epsilon}^o)^{\mathrm{T}} \rangle = \langle (\mathbf{A}H(\boldsymbol{\epsilon}^f) + \boldsymbol{\eta})\{\mathbf{A}H(\boldsymbol{\epsilon}^f) + \boldsymbol{\eta}\}^{\mathrm{T}} \rangle \cong \rho \mathbf{A}\mathbf{H}\mathbf{P}^f \mathbf{H}^{\mathrm{T}}\mathbf{A}^{\mathrm{T}} + \mathbf{R}^{uc} \text{ and} \tag{B8}$$

$$\mathbf{C} = \langle \boldsymbol{\epsilon}^f (\boldsymbol{\epsilon}^o)^{\mathrm{T}} \rangle = \langle \boldsymbol{\epsilon}^f \{\mathbf{A}H(\boldsymbol{\epsilon}^f) + \boldsymbol{\eta}\}^{\mathrm{T}} \rangle \cong \rho \mathbf{P}^f \mathbf{H}^{\mathrm{T}}\mathbf{A}^{\mathrm{T}}. \tag{B9}$$

Therefore, Eqs. (B4)–(B7) become

$$\langle \boldsymbol{d}^{o-b} (\boldsymbol{d}^{o-b})^{\mathrm{T}} \rangle = \rho (\mathbf{I}^{p\times p} - \mathbf{A})\mathbf{H}\mathbf{P}^f \mathbf{H}^{\mathrm{T}} (\mathbf{I}^{p\times p} - \mathbf{A})^{\mathrm{T}} + \mathbf{R}^{uc} , \tag{B10}$$

$$\langle \boldsymbol{d}^{a-b} (\boldsymbol{d}^{o-b})^{\mathrm{T}} \rangle = \rho \mathbf{H}\mathbf{P}^f \mathbf{H}^{\mathrm{T}} (\mathbf{I}^{p\times p} - \mathbf{A})^{\mathrm{T}} , \tag{B11}$$

$$\langle \boldsymbol{d}^{o-a} (\boldsymbol{d}^{o-b})^{\mathrm{T}} \rangle = -\rho \mathbf{A}\mathbf{H}\mathbf{P}^f \mathbf{H}^{\mathrm{T}} (\mathbf{I}^{p\times p} - \mathbf{A})^{\mathrm{T}} + \mathbf{R}^{uc} , \text{ and} \tag{B12}$$

$$\langle \boldsymbol{d}^{a-b} (\boldsymbol{d}^{o-a})^{\mathrm{T}} \rangle = -\rho \mathbf{H}\mathbf{P}^f \mathbf{H}^{\mathrm{T}}\mathbf{A}^{\mathrm{T}} + \mathbf{H}\acute{\mathbf{P}}^a \mathbf{H}^{\mathrm{T}} . \tag{B13}$$

Appendix C: Estimation of the parameters associated with the cross-correlation between forecast and observation errors

A diagonal element of Eq. (24) is represented as

$$\begin{aligned} \langle \boldsymbol{d}^{a-b} (\boldsymbol{d}^{o-b})^{\mathrm{T}} \rangle_{ii} &= \textstyle\sum_{j=1}^{p} \rho (\mathbf{H}\mathbf{P}^f \mathbf{H}^{\mathrm{T}})_{ij} (\mathbf{I} - \mathbf{A}^{est})^{\mathrm{T}}{}_{ji} \\ &= \textstyle\sum_{j=1}^{p} \rho (\mathbf{H}\mathbf{P}^f \mathbf{H}^{\mathrm{T}})_{ij} \delta_{ij} (1 - a_i^{est}) \\ &= \rho (\mathbf{H}\mathbf{P}^f \mathbf{H}^{\mathrm{T}})_{ii} (1 - a_i^{est}) \text{ , and therefore,} \end{aligned} \tag{C1}$$

$$a_i^{est} = 1 - \frac{\langle \boldsymbol{d}^{a-b} (\boldsymbol{d}^{o-b})^{\mathrm{T}} \rangle_{ii}}{\rho (\mathbf{H}\mathbf{P}^f \mathbf{H}^{\mathrm{T}})_{ii}} . \tag{C2}$$

Similarly, from Eq. (26),

$$\begin{aligned} \langle \boldsymbol{d}^{a-b} (\boldsymbol{d}^{o-a})^{\mathrm{T}} \rangle_{ii} &= -\textstyle\sum_{j=1}^{p} \rho \left(\mathbf{H}\mathbf{P}^f \mathbf{H}^{\mathrm{T}}\right)_{ij} \mathbf{A}_{ji}^{est} + \left(\mathbf{H}\acute{\mathbf{P}}^a \mathbf{H}^{\mathrm{T}}\right)_{ii} \\ &= -\textstyle\sum_{j=1}^{p} \rho \left(\mathbf{H}\mathbf{P}^f \mathbf{H}^{\mathrm{T}}\right)_{ij} \delta_{ij} a_i^{est} + \left(\mathbf{H}\acute{\mathbf{P}}^a \mathbf{H}^{\mathrm{T}}\right)_{ii} \\ &= -\rho \left(\mathbf{H}\mathbf{P}^f \mathbf{H}^{\mathrm{T}}\right)_{ii} a_i^{est} + \left(\mathbf{H}\acute{\mathbf{P}}^a \mathbf{H}^{\mathrm{T}}\right)_{ii} \text{ , and therefore,} \end{aligned} \tag{C3}$$

$$a_i^{est} = \frac{\left(\mathbf{H}\acute{\mathbf{P}}^a \mathbf{H}^{\mathrm{T}}\right)_{ii} - \langle \boldsymbol{d}^{a-b} (\boldsymbol{d}^{o-a})^{\mathrm{T}} \rangle_{ii}}{\rho (\mathbf{H}\mathbf{P}^f \mathbf{H}^{\mathrm{T}})_{ii}} . \tag{C4}$$

https://doi.org/10.5194/egusphere-2026-2653
Preprint. Discussion started: 11 June 2026

If $\mathbf{A}^{est} = a^{est}\mathbf{I}^{p\times p}$, Eqs. (C1) and (C2) originated from Eq. (24) become

$$tr[\langle \boldsymbol{d}^{a-b}(\boldsymbol{d}^{o-b})^{\mathrm{T}}\rangle] = \rho(1-a^{est})tr[\mathbf{H}\mathbf{P}^{f}\mathbf{H}^{\mathrm{T}}] \text{ and} \tag{C5}$$

$$a^{est} = 1 - \frac{tr\left[\langle \boldsymbol{d}^{a-b}(\boldsymbol{d}^{o-b})^{\mathrm{T}}\rangle\right]}{\rho\, tr[\mathbf{H}\mathbf{P}^{f}\mathbf{H}^{\mathrm{T}}]}, \tag{C6}$$

respectively, and Eqs. (C3) and (C4) from Eq. (26) become

$$tr[\langle \boldsymbol{d}^{a-b}(\boldsymbol{d}^{o-a})^{\mathrm{T}}\rangle] = -\rho a^{est} tr[\mathbf{H}\mathbf{P}^{f}\mathbf{H}^{\mathrm{T}}] + tr\left[\mathbf{H}\acute{\mathbf{P}}^{a}\mathbf{H}^{\mathrm{T}}\right] \text{ and} \tag{C7}$$

$$a^{est} = \frac{tr[\mathbf{H}\acute{\mathbf{P}}^{a}\mathbf{H}^{\mathrm{T}}] - tr[\langle \boldsymbol{d}^{a-b}(\boldsymbol{d}^{o-a})^{\mathrm{T}}\rangle]}{\rho\, tr[\mathbf{H}\mathbf{P}^{f}\mathbf{H}^{\mathrm{T}}]}. \tag{C8}$$

A diagonal element of Eq. (23) is represented as

$$\begin{aligned}\langle \boldsymbol{d}^{o-b}(\boldsymbol{d}^{o-b})^{\mathrm{T}}\rangle_{ii} &= \sum_{j=1}^{p}\sum_{k=1}^{p}\rho(\mathbf{I}^{p\times p} - \mathrm{A}^{est})_{ij}(\mathbf{H}\mathbf{P}^{f}\mathbf{H}^{\mathrm{T}})_{jk}(\mathbf{I}^{p\times p} - \mathbf{A}^{est})^{\mathrm{T}}{}_{ki} + \mathbf{R}^{uc}{}_{ii} \\ &= \sum_{j=1}^{p}\sum_{k=1}^{p}\rho\delta_{ij}(1-a_i^{est})(\mathbf{H}\mathbf{P}^{f}\mathbf{H}^{\mathrm{T}})_{jk}\delta_{ik}(1-a_i^{est}) + r_{\mathrm{i}}^{uc\_est} \\ &= \rho(1-a_i^{est})^2(\mathbf{H}\mathbf{P}^{f}\mathbf{H}^{\mathrm{T}})_{ii} + r_{\mathrm{i}}^{uc\_est}\text{, and therefore,}\end{aligned} \tag{C9}$$

$$r_{\mathrm{i}}^{uc\_est} = \langle \boldsymbol{d}^{o-b}(\boldsymbol{d}^{o-b})^{\mathrm{T}}\rangle_{ii} - \rho(1-a_i^{est})^2(\mathbf{H}\mathbf{P}^{f}\mathbf{H}^{\mathrm{T}})_{ii}\,. \tag{C10}$$

Substituting a_i^{est} in Eq. (C2) into Eq. (C10),

$$r_{\mathrm{i}}^{uc\_est} = \langle \boldsymbol{d}^{o-b}(\boldsymbol{d}^{o-b})^{\mathrm{T}}\rangle_{ii} - \left(\frac{\langle \boldsymbol{d}^{a-b}(\boldsymbol{d}^{o-b})^{\mathrm{T}}\rangle_{ii}}{\rho(\mathbf{H}\mathbf{P}^{f}\mathbf{H}^{\mathrm{T}})_{ii}}\right)^{2}\rho(\mathbf{H}\mathbf{P}^{f}\mathbf{H}^{\mathrm{T}})_{ii} = \langle \boldsymbol{d}^{o-b}(\boldsymbol{d}^{o-b})^{\mathrm{T}}\rangle_{ii} - \frac{\langle \boldsymbol{d}^{a-b}(\boldsymbol{d}^{o-b})^{\mathrm{T}}\rangle_{ii}^{2}}{\rho(\mathbf{H}\mathbf{P}^{f}\mathbf{H}^{\mathrm{T}})_{ii}}\,. \tag{C11}$$

Similarly, from Eq. (25),

https://doi.org/10.5194/egusphere-2026-2653
Preprint. Discussion started: 11 June 2026

$$\langle \boldsymbol{d}^{o-a}(\boldsymbol{d}^{o-b})^{\mathrm{T}}\rangle_{ii} = -\sum_{j=1}^{p}\sum_{k=1}^{p}\rho\mathbf{A}_{ij}(\mathbf{H}\mathbf{P}^{f}\mathbf{H}^{\mathrm{T}})_{jk}(\mathbf{I}^{p\times p}-\mathbf{A})^{\mathrm{T}}{}_{ki} + \mathbf{R}^{uc}{}_{ii}$$

$$= -\sum_{j=1}^{p}\sum_{k=1}^{p}\rho\delta_{ij}a_i^{est}(\mathbf{H}\mathbf{P}^{f}\mathbf{H}^{\mathrm{T}})_{jk}\delta_{ik}(1-a_i^{est}) + r_{\mathrm{i}}^{uc_{est}}$$

$$= -\rho a_i^{est}(\mathbf{H}\mathbf{P}^{f}\mathbf{H}^{\mathrm{T}})_{ii}(1-a_i^{est}) + r_{\mathrm{i}}^{uc\_est}\text{ , and therefore,} \quad \text{(C12)}$$

$$r_{\mathrm{i}}^{uc\_est} = \langle \boldsymbol{d}^{o-a}(\boldsymbol{d}^{o-b})^{\mathrm{T}}\rangle_{ii} + \rho a_i^{est}(\mathbf{H}\mathbf{P}^{f}\mathbf{H}^{\mathrm{T}})_{ii}(1-a_i^{est})\,. \quad \text{(C13)}$$

Substituting a_i^{est} in Eq. (C2) into Eq. (C13),

$$r_{\mathrm{i}}^{uc\_est} = \langle \boldsymbol{d}^{o-a}(\boldsymbol{d}^{o-b})^{\mathrm{T}}\rangle_{ii} + \left(1-\frac{\langle \boldsymbol{d}^{a-b}(\boldsymbol{d}^{o-b})^{\mathrm{T}}\rangle_{ii}}{\rho(\mathbf{H}\mathbf{P}^{f}\mathbf{H}^{\mathrm{T}})_{ii}}\right)\rho(\mathbf{H}\mathbf{P}^{f}\mathbf{H}^{\mathrm{T}})_{ii}\frac{\langle \boldsymbol{d}^{a-b}(\boldsymbol{d}^{o-b})^{\mathrm{T}}\rangle_{ii}}{\rho(\mathbf{H}\mathbf{P}^{f}\mathbf{H}^{\mathrm{T}})_{ii}}$$

$$= \langle \boldsymbol{d}^{o-a}(\boldsymbol{d}^{o-b})^{\mathrm{T}}\rangle_{ii} + \langle \boldsymbol{d}^{a-b}(\boldsymbol{d}^{o-b})^{\mathrm{T}}\rangle_{ii} - \frac{\langle \boldsymbol{d}^{a-b}(\boldsymbol{d}^{o-b})^{\mathrm{T}}\rangle_{ii}{}^{2}}{\rho(\mathbf{H}\mathbf{P}^{f}\mathbf{H}^{\mathrm{T}})_{ii}}$$

$$= \langle \boldsymbol{d}^{o-b}(\boldsymbol{d}^{o-b})^{\mathrm{T}}\rangle_{ii} - \frac{\langle \boldsymbol{d}^{a-b}(\boldsymbol{d}^{o-b})^{\mathrm{T}}\rangle_{ii}{}^{2}}{\rho(\mathbf{H}\mathbf{P}^{f}\mathbf{H}^{\mathrm{T}})_{ii}}\,. \quad \text{(C14)}$$

Therefore, $r_{\mathrm{i}}^{uc\_est}$ of Eqs. (C11) and (C14) are consistent with each other.

Substituting a_i^{est} in Eq. (C4) into Eqs. (C10) and (C13), two kinds of $r_{\mathrm{i}}^{uc\_est}$ are derived as

$$r_i^{uc\_est} = \langle \boldsymbol{d}^{o-b}(\boldsymbol{d}^{o-b})^{\mathrm{T}}\rangle_{ii} - \rho(\mathbf{H}\mathbf{P}^{f}\mathbf{H}^{\mathrm{T}})_{ii}\left[1-\frac{(\mathbf{H}\acute{\mathbf{P}}^{a}\mathbf{H}^{\mathrm{T}})_{ii}-\langle \boldsymbol{d}^{a-b}(\boldsymbol{d}^{o-a})^{\mathrm{T}}\rangle_{ii}}{\rho(\mathbf{H}\mathbf{P}^{f}\mathbf{H}^{\mathrm{T}})_{ii}}\right]^{2} \text{ and} \quad \text{(C15)}$$

$$r_i^{uc\_est} = \langle \boldsymbol{d}^{o-a}(\boldsymbol{d}^{o-b})^{\mathrm{T}}\rangle_{ii} + \left[(\mathbf{H}\acute{\mathbf{P}}^{a}\mathbf{H}^{\mathrm{T}})_{ii} - \langle \boldsymbol{d}^{a-b}(\boldsymbol{d}^{o-a})^{\mathrm{T}}\rangle_{ii}\right]\left[1-\frac{(\mathbf{H}\acute{\mathbf{P}}^{a}\mathbf{H}^{\mathrm{T}})_{ii}-\langle \boldsymbol{d}^{a-b}(\boldsymbol{d}^{o-a})^{\mathrm{T}}\rangle_{ii}}{\rho(\mathbf{H}\mathbf{P}^{f}\mathbf{H}^{\mathrm{T}})_{ii}}\right], \quad \text{(C16)}$$

respectively.

If $\mathbf{A}^{est} = a^{est}\mathbf{I}^{p\times p}$ and $\mathbf{R}^{uc\_est} = r^{uc\_est}\mathbf{I}^{p\times p}$, Eqs. (C10) and (C13) become

$$r^{uc\_est} = \frac{1}{p}\{tr[\langle \boldsymbol{d}^{o-b}(\boldsymbol{d}^{o-b})^{\mathrm{T}}\rangle] - \rho(1-a^{est})^{2}tr[\mathbf{H}\mathbf{P}^{f}\mathbf{H}^{\mathrm{T}}]\} \text{ and} \quad \text{(C17)}$$

$$r^{uc\_est} = \frac{1}{p}\{tr[\langle \boldsymbol{d}^{o-a}(\boldsymbol{d}^{o-b})^{\mathrm{T}}\rangle] + \rho a^{est}(1-a^{est})tr[\mathbf{H}\mathbf{P}^{f}\mathbf{H}^{\mathrm{T}}]\}\,. \quad \text{(C18)}$$

Substituting a^{est} of Eq. (C6) into Eqs. (C17) and (C18), a single consistent r^{uc_est} is estimated from

https://doi.org/10.5194/egusphere-2026-2653
Preprint. Discussion started: 11 June 2026

$$r^{uc\_est} = \frac{1}{p}\left\{ tr[\langle \boldsymbol{d}^{o-b}(\boldsymbol{d}^{o-b})^{\mathrm{T}}\rangle] - \frac{tr\left[\langle \boldsymbol{d}^{a-b}(\boldsymbol{d}^{o-b})^{\mathrm{T}}\rangle\right]^2}{\rho\, tr[\mathbf{H}\mathbf{P}^f\mathbf{H}^{\mathrm{T}}]} \right\}. \tag{C19}$$

Substituting a^{est} of Eq. (C8) into Eqs. (C17) and (C18), two types of r^{uc_est} are derived as

$$r^{uc\_est} = \frac{1}{p}\left\{ tr[\langle \boldsymbol{d}^{o-b}(\boldsymbol{d}^{o-b})^{\mathrm{T}}\rangle] - \rho\, tr[\mathbf{H}\mathbf{P}^f\mathbf{H}^{\mathrm{T}}]\left[1 - \frac{tr[\mathbf{H}\acute{\mathbf{P}}^a\mathbf{H}^{\mathrm{T}}] - tr[\langle \boldsymbol{d}^{a-b}(\boldsymbol{d}^{o-a})^{\mathrm{T}}\rangle]}{\rho\, tr[\mathbf{H}\mathbf{P}^f\mathbf{H}^{\mathrm{T}}]}\right]^2 \right\} \text{ and} \tag{C20}$$

$$r^{uc\_est} = \frac{1}{p}\left\{ tr[\langle \boldsymbol{d}^{o-a}(\boldsymbol{d}^{o-b})^{\mathrm{T}}\rangle] + \left[tr\left[\mathbf{H}\acute{\mathbf{P}}^a\mathbf{H}^{\mathrm{T}}\right] - tr[\langle \boldsymbol{d}^{a-b}(\boldsymbol{d}^{o-a})^{\mathrm{T}}\rangle]\right]\left[1 - \frac{tr[\mathbf{H}\acute{\mathbf{P}}^a\mathbf{H}^{\mathrm{T}}] - tr[\langle \boldsymbol{d}^{a-b}(\boldsymbol{d}^{o-a})^{\mathrm{T}}\rangle]}{\rho\, tr[\mathbf{H}\mathbf{P}^f\mathbf{H}^{\mathrm{T}}]}\right] \right\}, \tag{C21}$$

respectively.

Code and data availability

The source codes and datasets used in this study are available at https://doi.org/10.5281/zenodo.15430272.

Author contributions

YK conceived the study, developed the methodology, performed the analysis and investigation, curated the data, developed the software, and prepared the original draft with visualization. SO contributed to the study design and methodology, developed the software, supervised the project, acquired funding, administered the project, and reviewed and edited the manuscript. TM contributed to the study design, acquired funding, administered the project, supervised the research, and reviewed and edited the manuscript. All authors validated the results and approved the final manuscript.

Competing interests

TM is a member of the editorial board of Nonlinear Processes in Geophysics.

Financial support

This work was supported by the COE research grant in computational science from Hyogo Prefecture and Kobe City through Foundation for Computational Science; the Japan Aerospace Exploration Agency (EORA3: RA3MAF001 and EORA4: ER4MAF004); JSPS KAKENHI (Grant Numbers JP23K13174, JP24H00021, and JP24H02227); JST CREST (Grant

https://doi.org/10.5194/egusphere-2026-2653
Preprint. Discussion started: 11 June 2026

Numbers JPMJSA2109 and JPMJCR24Q3); the RIKEN TRIP initiative (RIKEN Prediction Science); the UK Advanced Research + Invention Agency (ARIA) under project FPCW-PR01-P007; MAthematics-based Creation of Science Program.

References

Bishop, Craig H., Brian J. Etherton, and Sharanya J. Majumdar. *Adaptive Sampling with the Ensemble Transform Kalman Filter. Part I: Theoretical Aspects*. Monthly Weather Review. March 1, 2001. https://doi.org/10.1175/1520-0493(2001)129<0420:ASWTET>2.0.CO;2.

Desroziers, G., L. Berre, B. Chapnik, and P. Poli. "Diagnosis of Observation, Background and Analysis-Error Statistics in Observation Space." *Quarterly Journal of the Royal Meteorological Society* 131, no. 613 (2005): 3385–96. https://doi.org/10.1256/qj.05.108.

Hirose, Fuyuki, Kenji Maeda, and Osamu Kamigaichi. "Tidal Forcing of Interplate Earthquakes Along the Tonga-Kermadec Trench." *Journal of Geophysical Research: Solid Earth* 124, no. 10 (2019): 10498–521. https://doi.org/10.1029/2019JB018088.

Hoover, Brett T., and Rolf H. Langland. "Forecast and Observation-Impact Experiments in the Navy Global Environmental Model with Assimilation of ECWMF Analysis Data in the Global Domain." *Journal of the Meteorological Society of Japan. Ser. II* 95, no. 6 (2017): 369–89. https://doi.org/10.2151/jmsj.2017-023.

Kido, Shoichiro, Masami Nonaka, and Yasumasa Miyazawa. "JCOPE-FGO: An Eddy-Resolving Quasi-Global Ocean Reanalysis Product." *Ocean Dynamics* 72, no. 8 (2022): 599–619. https://doi.org/10.1007/s10236-022-01521-z.

Lorenz, Edward N. "Predictability: A Problem Partly Solved." *Proceedings of the Seminar on Predictability, Vol. 1* (Reading, Berkshire, UK), 1996, 1–18.

Lorenz, Edward N., and Kerry A. Emanuel. *Optimal Sites for Supplementary Weather Observations: Simulation with a Small Model*. Journal of the Atmospheric Sciences. February 1, 1998. https://doi.org/10.1175/1520-0469(1998)055<0399:OSFSWO>2.0.CO;2

Ohishi, Shun, Yuki Kobayashi, and Takemasa Miyoshi. "Including Cross Correlation between Forecast and Observation Errors in an Ensemble Kalman Filter." Monthly Weather Review. *Monthly Weather Review* 153, no. 6 (2025): 1035–43. https://doi.org/10.1175/MWR-D-25-0016.1.